NASA TN D-290



# TECHNICAL NOTE

D-290

## PHOTOMICROGRAPHIC TRACKING OF ETHANOL DROPS IN A ROCKET CHAMBER BURNING ETHANOL AND LIQUID OXYGEN

By Robert D. Ingebo

Lewis Research Center
Cleveland, Ohio

NATIONAL AERONAUTICS AND SPACE ADMINISTRATION

WASHINGTON June 1960

NATIONAL AERONAUTICS AND SPACE ADMINISTRATION

TECHNICAL NOTE D-290

# PHOTOMICROGRAPHIC TRACKING OF ETHANOL DROPS IN A ROCKET CHAMBER BURNING ETHANOL AND LIQUID OXYGEN

By Robert D. Ingebo



## SUMMARY

An ultra-high-speed tracking camera was developed at NASA Lewis Research Center to photograph ethanol sprays accelerating and burning in a 2-inch-diameter by 16-inch-length rocket combustor with liquid oxygen as the oxidant. Thus, drop-size-distribution data for the breakup of ethanol jets inside the combustor were obtained from photomicrographs of the spray taken 4 inches downstream from the injector face.

Analyses of the drop-size-distribution data with the Nukiyama-Tanasawa and log-probability expressions gave volume-median drop diameters of 154 and 158 microns, respectively, which agreed well with the value of 152 microns obtained by direct integration of the data. However, the Rosin-Rammler expression gave a considerably lower value of 116 microns. The maximum observed drop size was 344 microns.

Ethanol jets were injected into the combustion chamber at a velocity of approximately 25 feet per second, and drop-velocity data were obtained for the fuel spray by tracking the drops with a rotating mirror during an exposure time of approximately 8 microseconds. Velocities were found to be approximately 30 feet per second for 344-micron-diameter drops, and 70 feet per second for 35-micron-diameter drops.

## INTRODUCTION

The combustion of fuel sprays in a rocket chamber may be studied by determining the size and velocity of the burning drops. From such data, it is possible to calculate drop vaporization and acceleration rates. Knowledge of such rates is useful in application to the design, operation, and performance of combustors (ref. 1).

In order to determine the size and velocity of ethanol drops in a rocket chamber burning ethanol and liquid oxygen, an ultra-high-speed tracking camera was developed at NASA Lewis Research Center. One of the

most difficult problems encountered in photographing burning sprays was that of providing sufficient illumination of the spray to obtain clear drop images on the film. Similar difficulties have been encountered by other investigators (ref. 2). However, use of an improved light source and a red filter, in combination with infrared film, produced photomicrographs of the desired quality.

Photomicrographs of burning ethanol sprays formed by breakup of single jets of fuel were taken in a low-thrust (2-in.-diam.) rocket chamber, 4 inches downstream from the injector face. Pictures taken closer to the injector (1 to 3 in. away) gave poorly defined drop images. From the photomicrographs, drop-size-distribution data were obtained and analyzed using the Nukiyama-Tanasawa and log-probability expressions for size distributions (ref. 3).



## SYMBOLS

The following symbols appear in this report:

b constant (eq. (1))

D drop diameter, cm

$\overline{D}$ size parameter in eq. (4), cm

D* drop diameter at R = 0.50, cm

$D_{30}$ volume-median drop diameter, defined by the general expression:

$$(D_{ef})^{e-f} = \frac{\sum nD^e}{\sum nD^f} \quad \text{which gives} \quad D_{30} = \left(\frac{\sum nD^3}{\sum n}\right)^{1/3}$$

e mean-diameter notation

f mean-diameter notation

L distance from tracking mirror to film plane, cm

M magnification

n number of drops

q constant (eq. (4))

R volume fraction of drops having diameters < D

$\Delta R$ $nD^3 / \sum_{D=0}^{D=max.} nD^3$

$V_d$ drop velocity, ft/sec

$y$ $\ln(D/D^*)$

$\delta$ constant (eq. (3))

$\omega$ tracking-mirror speed, rps



## APPARATUS AND PROCEDURE

The size and velocity of ethanol drops were determined photomicrographically by tracking them inside the rocket combustor shown in figure 1. The 2-inch-inside-diameter by 16-inch-length combustor assembly included the injector, nozzle, chamber spacers, and window section with nitrogen-cooled stubs. Pyrex glass, 1/2-inch thick and 2 inches in diameter, was used for the windows.

The injector shown in figure 2 consisted of two rows of 0.032-inch-diameter orifices, twelve in each row, for introducing jets of ethanol (95 percent, and 5 percent water). Two 0.089-inch-inside-diameter stainless-steel tubes were used for introducing impinging jets of liquid oxygen, which formed a sheet parallel to and centered in between the rows of fuel jets. The nozzle-throat diameter was 0.75 inch.

A program timer was used for each 2-second-duration test firing, and photomicrographs were taken in the middle of the run, approximately 1 second after ignition. A liquid-nitrogen bath was used to cool the firing valve and liquid-oxygen supply tank. The pressurized-tank feed system gave propellant flows of 0.126 and 0.164±0.004 pound per second of liquid oxygen and ethanol, respectively. Ethanol jets were injected into the chamber at a velocity of approximately 25 feet per second. The oxidant-fuel weight ratio was 0.77±0.04, and the chamber pressure was 82±2 pounds per square inch gage. An average characteristic-exhaust velocity $c^*$ of 4750±200 was obtained, which gave a $c^*$ efficiency of approximately 100 percent (102±4 percent). Variation in propellant flow and chamber pressure between test firings, approximately 1000 tests in all, gave the variation of 4 percent for calculated values. Chamber pressure was measured from a static tap at the injector face with a Bourdon-tube instrument having an accuracy of ±1 pound per square inch gage. Propellant flow rates were measured with rotating-vane-type meters having accuracies of ±1 percent.

The camera shown in figure 1 was an improved model of the camera described in reference 4. Since the luminosity of the flame was relatively low in comparison with the intensity of the light source, the flame light did not present a problem in exposing the film. However, because of the opacity of the flame, it was necessary to increase the intensity of the light source by adding another pair of 1-microfarad (20,000-volt) condensers to obtain a total capacity of 4 microfarads. Also, pressurizing the magnesium spark gap with argon gas at 30 pounds per square inch gage increased the intensity of the light source in the long wavelengths. By using $9\frac{1}{2}$-inch-width infrared aerial film in combination with a Wratten No. 25 red filter on the light source, it was possible to utilize long-wavelength light that gave relatively little scattering in the spray and thereby produced high-contrast negatives. All lenses were commercial type with f-numbers and focal lengths as shown in figure 3. An additional objective lens (14-in. focal length, f/6.3) was used to replace the one shown in figure 3 when the magnification was changed to six times. Figure 4 shows a circuit diagram of the electronic equipment used to synchronize the light-source flash with the tracking mirror. The mirror face had to be at an angle of approximately $45^{\circ}$ to the film plane and the projection lens when the flash occurred.

The correct mirror speeds were determined by first taking pictures at a relatively low mirror speed with a Polaroid Film camera. From the streaks left by the large drop images on the film, it was possible to estimate the correct mirror speed for stopping the large drop images although contrast was poor. Thus, the mirror speed was increased by steps until the large drop images were stopped (although small drop images were not stopped). By gradually stepping up the mirror speed and using infrared film for a series of tests, it was possible to stop large drop images at relatively low mirror speeds, and small drop images (with some streaking of the large drops) at higher mirror speeds.

Photomicrographs were taken at the chamber centerline, 4 inches from the injector face, as shown in figure 5(a). This was in the plane of the liquid-oxygen sheet (see fig. 2), and no drop images appeared. However, in the plane of the row of fuel jets near the camera objective lens, the ethanol drops are clearly visible as shown in figure 5(b). Figure 5(c) shows mostly flame in between the liquid-oxygen and fuel planes. A magnification of 6 was used for these pictures.

Drop-size-distribution measurements were made from photomicrographs similar to that shown in figure 6. A magnification of 15 was used for these pictures. Drop-diameter measurements were made with an accuracy of $\pm 5$ microns, and drop velocities were calculated from the camera mirror speeds with an accuracy of $\pm 5$ feet per second. Forty pictures were taken, and 1110 drops were measured for the total drop-size count.

## RESULTS AND DISCUSSION

From the photomicrographs of burning ethanol drops taken at a distance of 4 inches downstream from the injector face, it was possible to determine the size distribution of the drops and analyze the data using the Nukiyama-Tanasawa, log-probability, and Rosin-Rammler expressions for size distribution. Also, drop velocities were determined from the speed at which the mirror tracked the drops in stopping their images on the infrared film.

The velocity $V_d$ of a stopped ethanol-drop image (as shown in fig. 6) was calculated from the expression $V_d = 4\pi L\omega/M$ where $L$ is the distance from the mirror to the film plane, $M$ is the magnification ($M = 15$), and $\omega$ is the mirror speed. A semilog plot of the observed drop velocity against the drop diameter, at a distance 4 inches downstream from the injector face, is shown in figure 7. The injection velocity for the ethanol jets was approximately 25 feet per second, whereas drop velocities were found to be approximately 30 and 70 feet per second for the 344- and 35-micron-diameter drops, respectively, at the camera station.

The drop count, at a distance 4 inches downstream from the injector face, is given in table I. Here, the volume-median drop diameter $D_{30}$ was found to be 152 microns as calculated by direct integration of the experimental drop-size data. This agrees with the value of 154 microns obtained for $D_{30}$ from figure 8, which shows a plot of the following Nukiyama-Tanasawa expression:

$$\frac{dR}{dD} = \frac{b^6}{120} D^5 e^{-bD} \tag{1}$$

which may be rewritten as follows:

$$\log \frac{\Delta R}{(\Delta D)D^5} = -1.7\left(\frac{D}{D^{30}}\right) + \log\left[\left(\frac{3.915}{D^{30}}\right)^6 \Big/ 120\right] \tag{2}$$

since integration of equation (1) gives $D_{30} = 3.915/b = -1.7/\text{slope}$.

The drop-size data were also plotted, as shown in figure 9, using the log-probability expression

$$R = \frac{\delta}{\sqrt{\pi}} \int_{-\infty}^{\delta y} e^{-\delta^2 y^2} dy \tag{3}$$

where $y = \ln(D/D^*)$. Integration of equation (3) and the slope of the plot in figure 9 gives a value of $D_{30}$ of 158 microns, which also agrees fairly well with the value obtained by direct integration of the drop-size data.

A plot of the Rosin-Rammler expression

$$1 - R = e^{-(D/\bar{D})^q} \tag{4}$$

shown in figure 10, gives a $D_{30}$ value of 116 microns. This is considerably below the value of 152 microns obtained by direct integration of the drop-size data. Thus, the Rosin-Rammler expression appeared to give the poorest results. However, more experimental drop-size data for fuel sprays burning in rocket combustors are needed to establish the general applicability of the Nukiyama-Tanasawa and log-probability expressions to burning sprays.

## CONCLUDING REMARKS

The most difficult problem encountered in photographing the fuel spray was that of providing sufficient light to penetrate the relatively opaque flame without scattering appreciably and still operate on an extremely short time scale (ten billionths of a second for a 10-micron-diam. drop traveling 100 ft/sec and magnified 15 times). However, with the tracking camera it was possible to have an exposure time of approximately 8 microseconds. Since long-wavelength light gave less light scattering, it was found that infrared film used in conjunction with a red filter on the light source gave the best results.

Lewis Research Center
National Aeronautics and Space Administration
Cleveland, Ohio, March 15, 1960

## REFERENCES

1. Clarke, J. S.: The Relation of Specific Heat Release to Pressure Drop in Aero-Gas-Turbine Combustion Chambers. Sec. 5: Gas Turbines. The Inst. Mech. Eng. (London), and ASME Joint Conf. on Combustion, 1955, pp. 24-31.

2. Rossman, Theodor G.: A High-Speed and High-Resolution Photographic Technique for the Observation of Propellants Injected into a Firing Combustion Chamber. Rep. 8007-981-008, Bell Aircraft Corp., May 18, 1959.

3. Mugele, R. A., and Evans, H. D.: Droplet Size Distribution in Sprays. Ind. and Eng. Chem., vol. 43, no. 6, June 1951, p. 1317.

4. Ingebo, Robert D.: Vaporization Rates and Drag Coefficients for Isooctane Sprays in Turbulent Air Streams. NACA TN 3265, 1954.

TABLE I. - DROP-SIZE-DISTRIBUTION DATA

[4 in. downstream from injector face.]

| Drop diameter, D, microns | | Number of drops, n | $\frac{\Delta R, \ nD^3}{\sum_{D=0}^{D=max.} nD^3}$ | R, percent |
|---|---|---|---|---|
| Range | Average | | | |
| 0-15 | 8 | 38 | $0.5 \times 10^4$ | 0.00 |
| 15-29 | 22 | 41 | 1.1 | .01 |
| 29-43 | 36 | 49 | 5.8 | .07 |
| 43-57 | 50 | 51 | 16.1 | .23 |
| 57-71 | 64 | 59 | 39.0 | .62 |
| 71-85 | 78 | 70 | 83.8 | 1.46 |
| 85-99 | 92 | 82 | 161.1 | 3.07 |
| 99-113 | 106 | 92 | 276.6 | 5.83 |
| 113-127 | 120 | 102 | 444.9 | 10.29 |
| 127-141 | 134 | 98 | 595.2 | 16.24 |
| 141-155 | 148 | 97 | 793.7 | 24.17 |
| 155-169 | 162 | 80 | 858.5 | 32.76 |
| 169-183 | 176 | 71 | 977.0 | 42.53 |
| 183-197 | 190 | 51 | 882.9 | 51.36 |
| 197-211 | 204 | 32 | 685.7 | 58.21 |
| 211-225 | 218 | 24 | 627.6 | 64.49 |
| 225-239 | 232 | 19 | 598.9 | 70.48 |
| 239-253 | 246 | 16 | 601.2 | 76.49 |
| 253-267 | 260 | 10 | 443.6 | 80.93 |
| 267-281 | 274 | 8 | 415.4 | 85.08 |
| 281-295 | 288 | 5 | 301.5 | 88.10 |
| 295-309 | 302 | 6 | 417.1 | 92.27 |
| 309-323 | 316 | 5 | 398.2 | 96.25 |
| 323-337 | 330 | 3 | 272.1 | 98.97 |
| 337-351 | 344 | 1 | 102.7 | 100.00 |

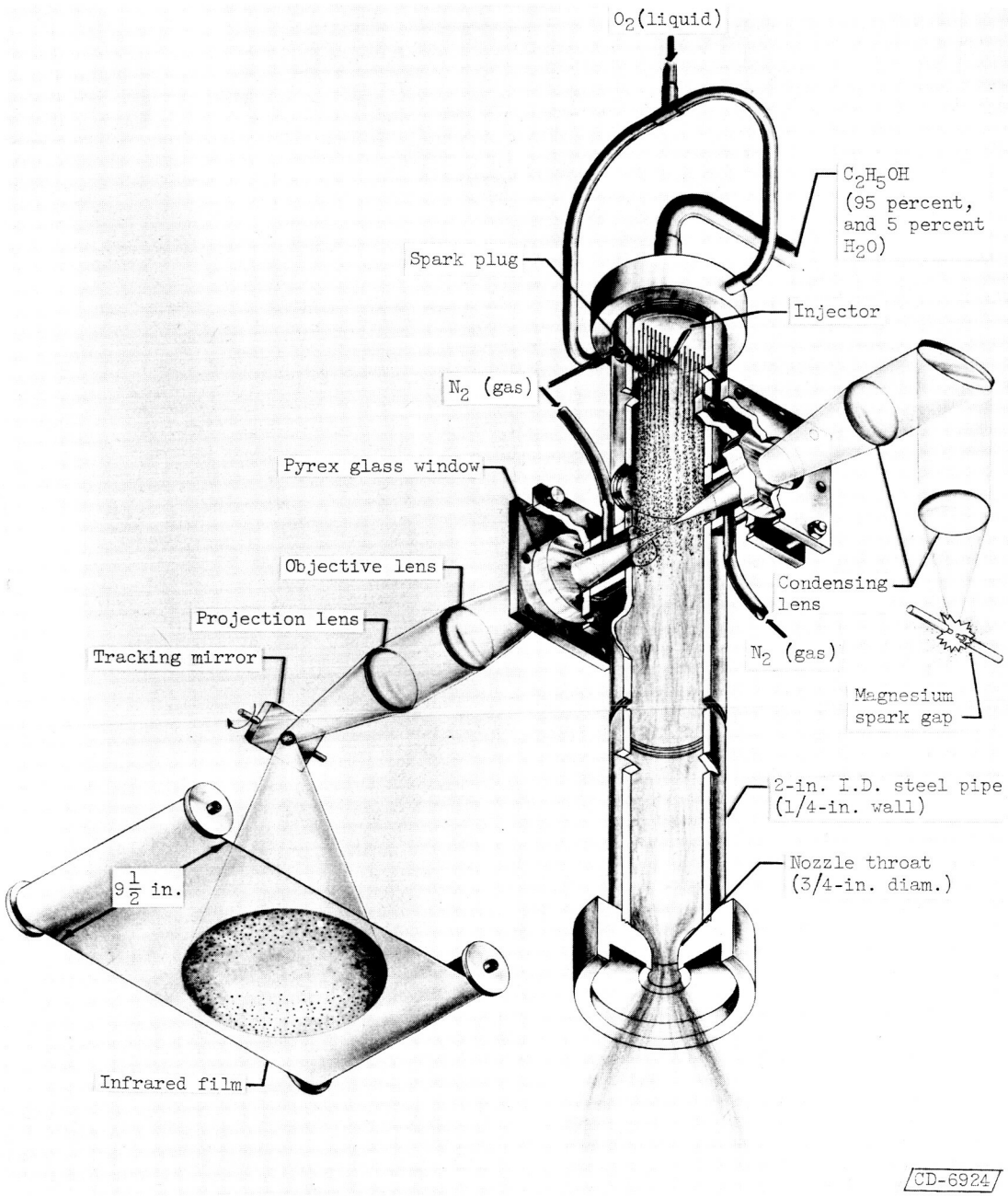


Figure 1. - Rocket chamber and camera equipment.

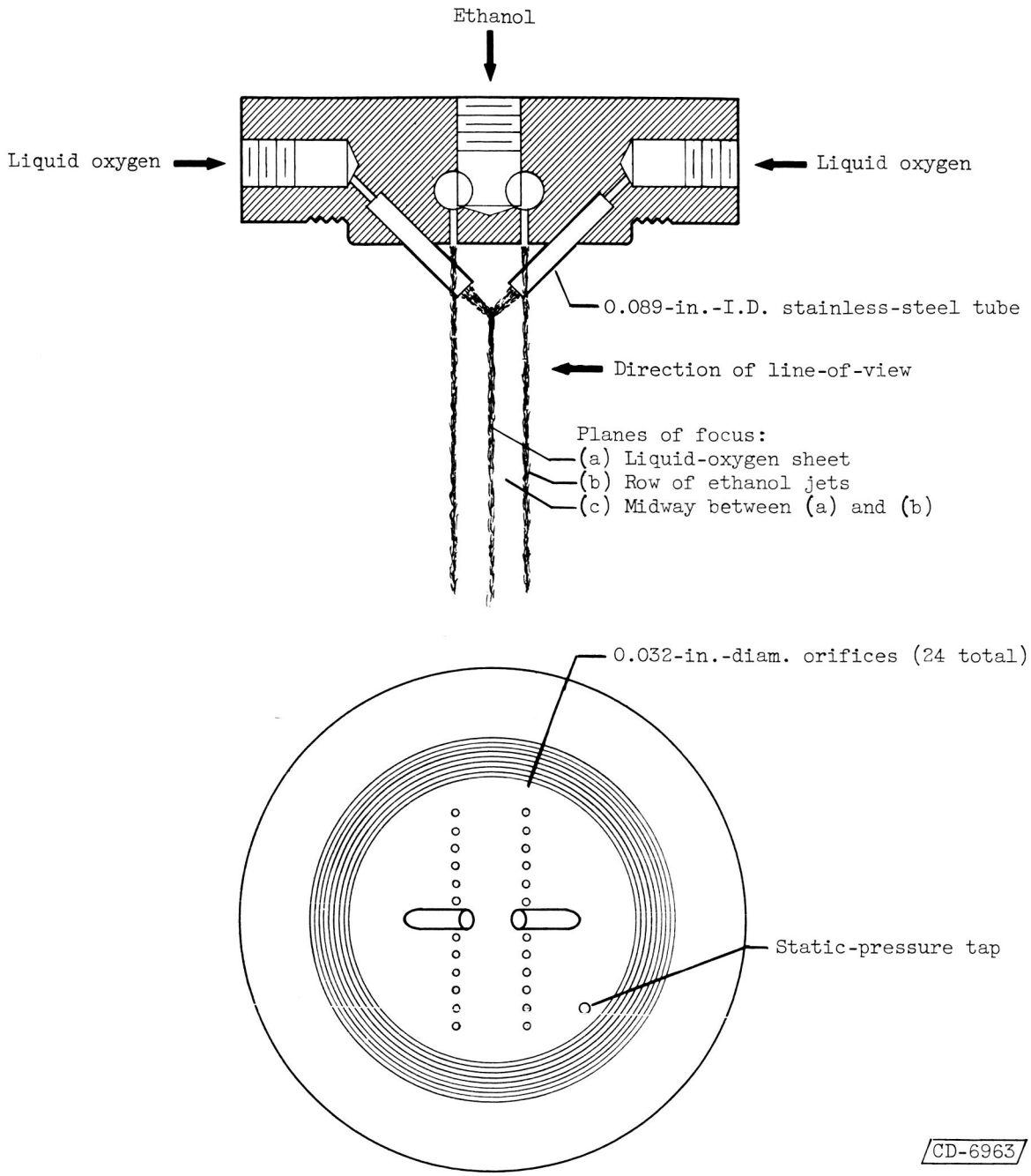


Figure 2. - Detail of propellant injector and planes photographed in figure 5.

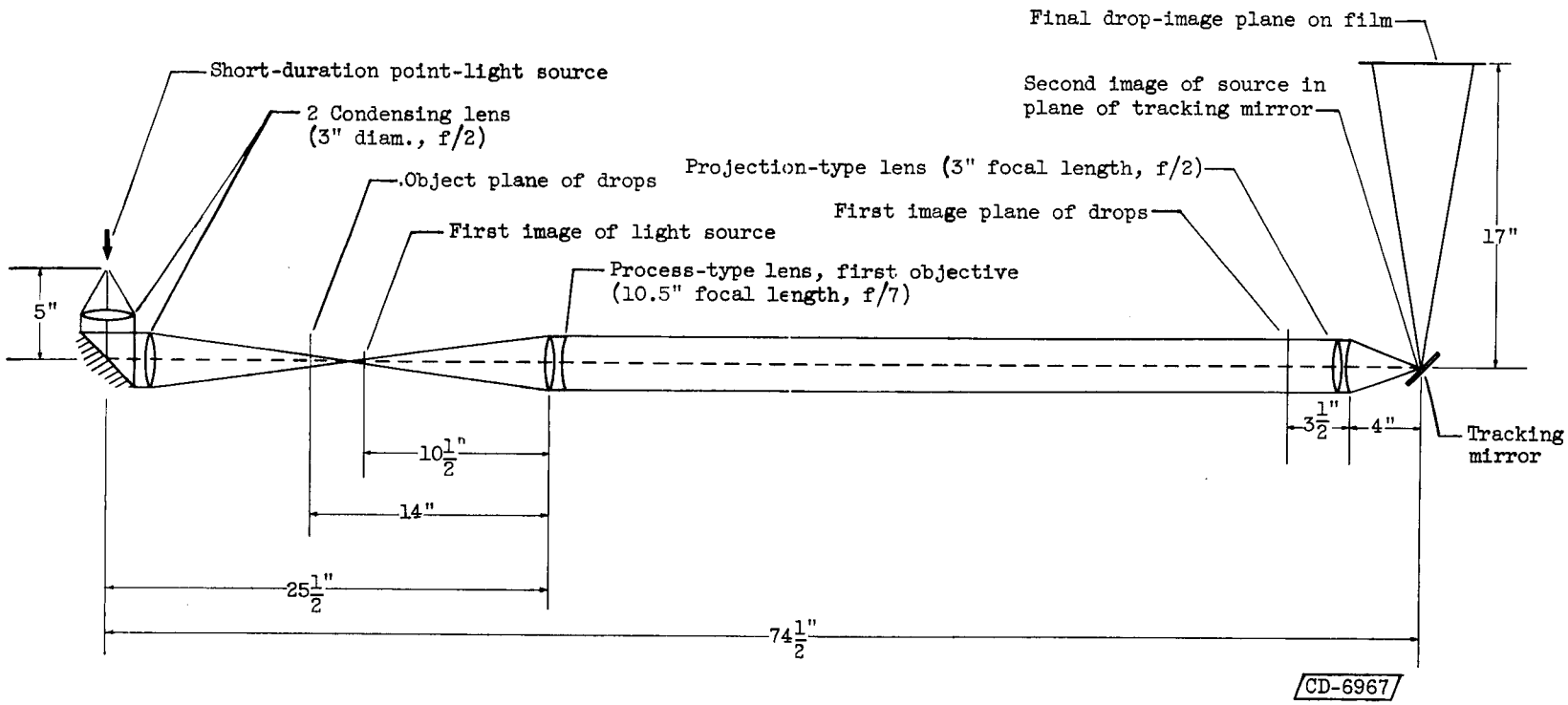


Figure 3. - Tracking-camera lens system; X15.

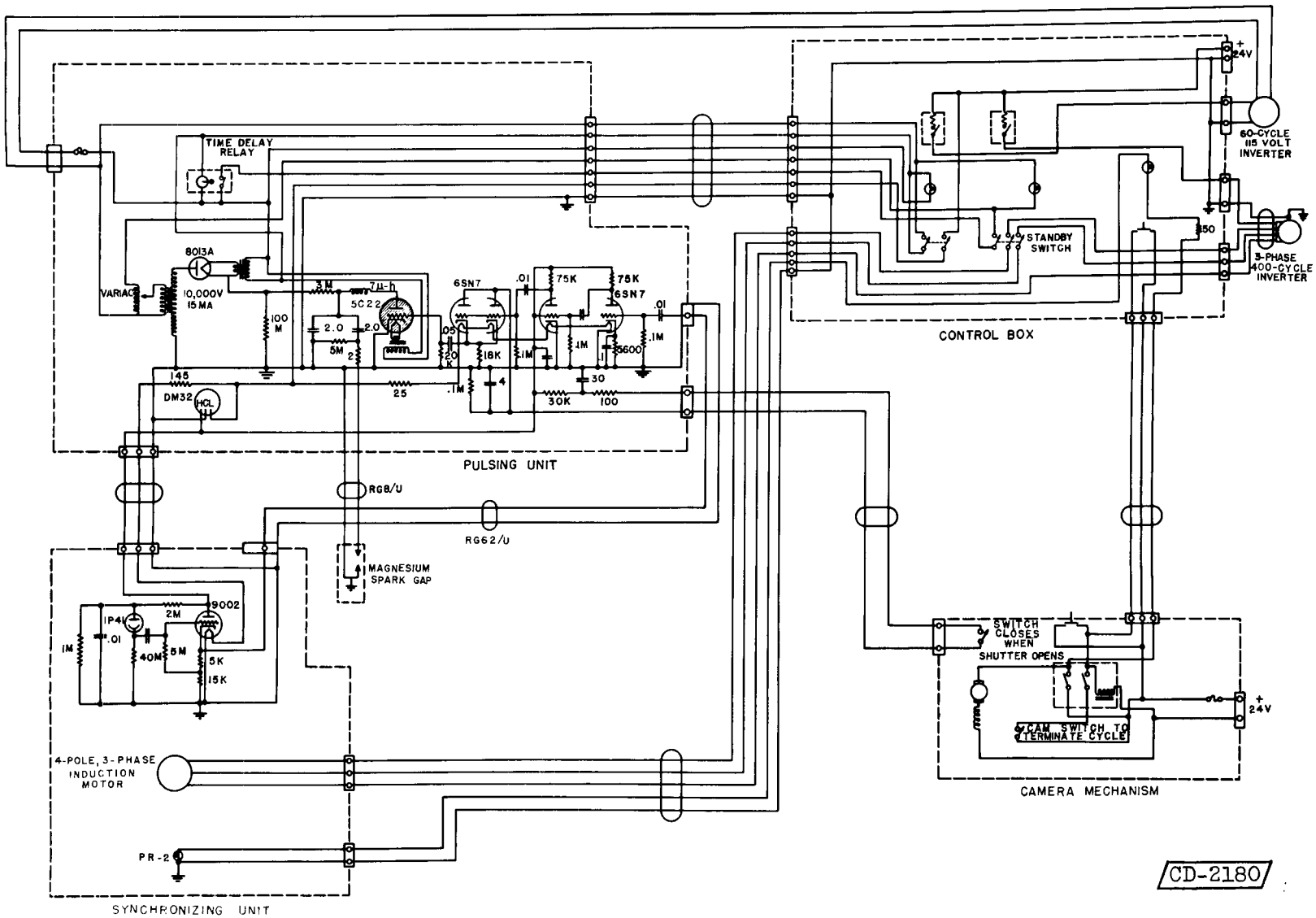


Figure 4. - Circuit diagram of electronic equipment for synchronizing light source with tracking mirror.

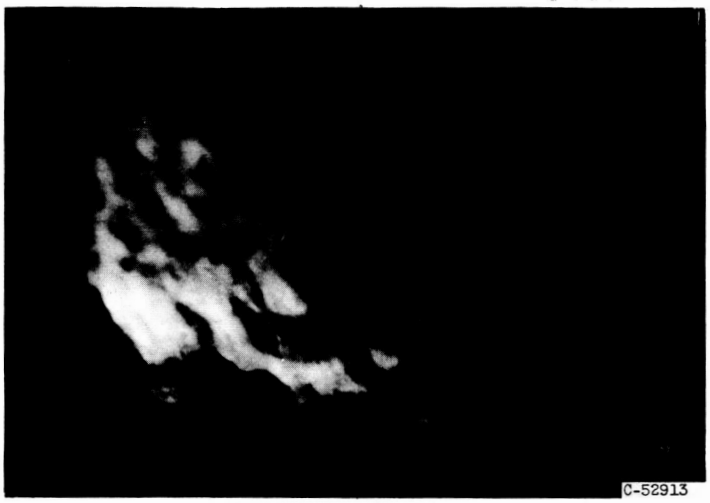


(a) In plane of liquid-oxygen sheet.

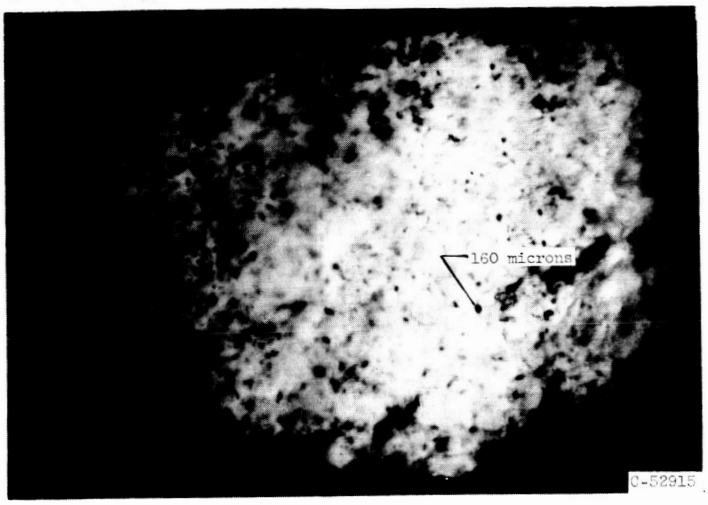


(b) In plane of fuel jets.


(c) In between planes of fuel and oxidant.

Figure 5. - Photomicrographs of spray; X6.

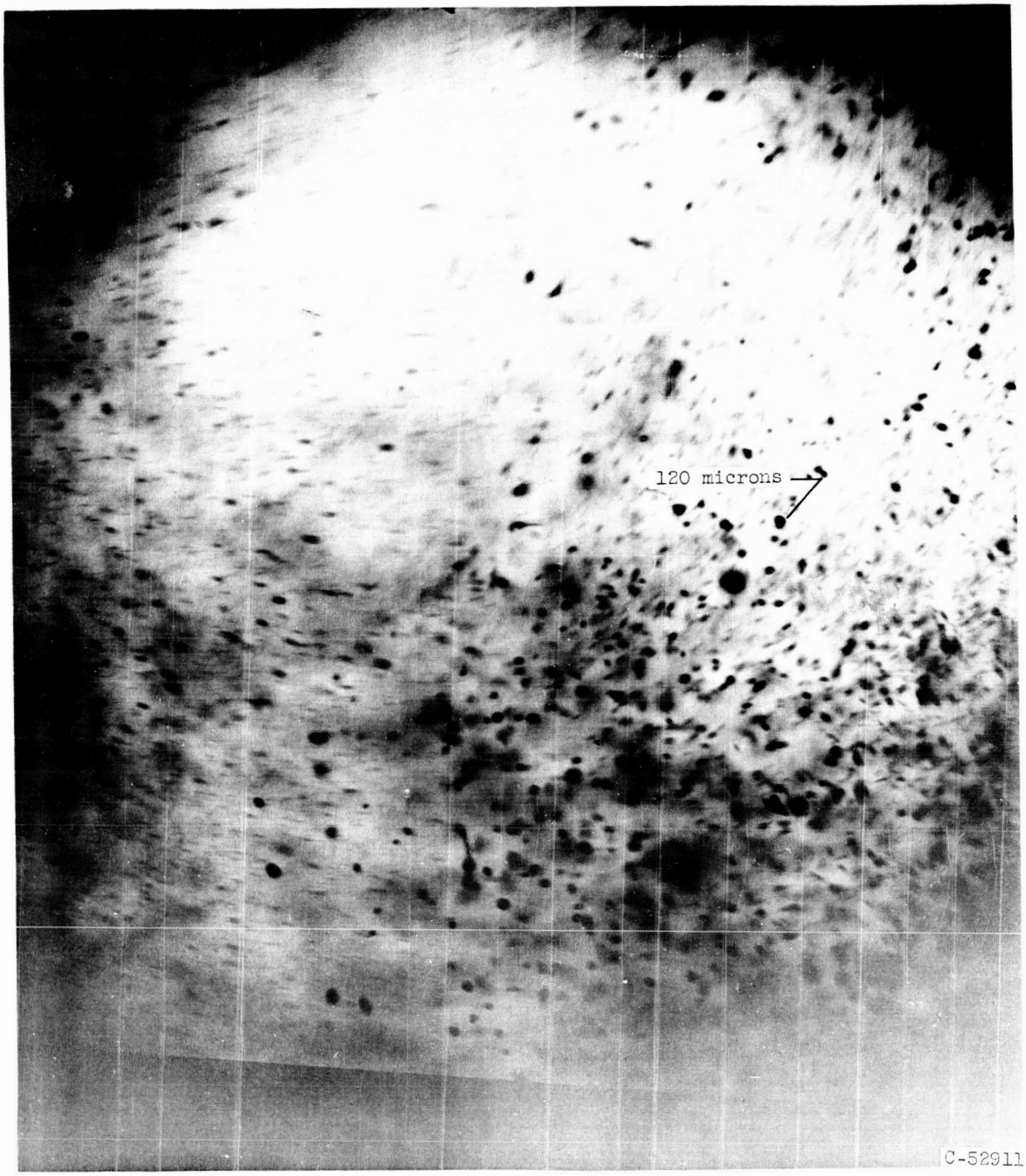


Figure 6. - Photomicrograph in plane of fuel jets; X15.

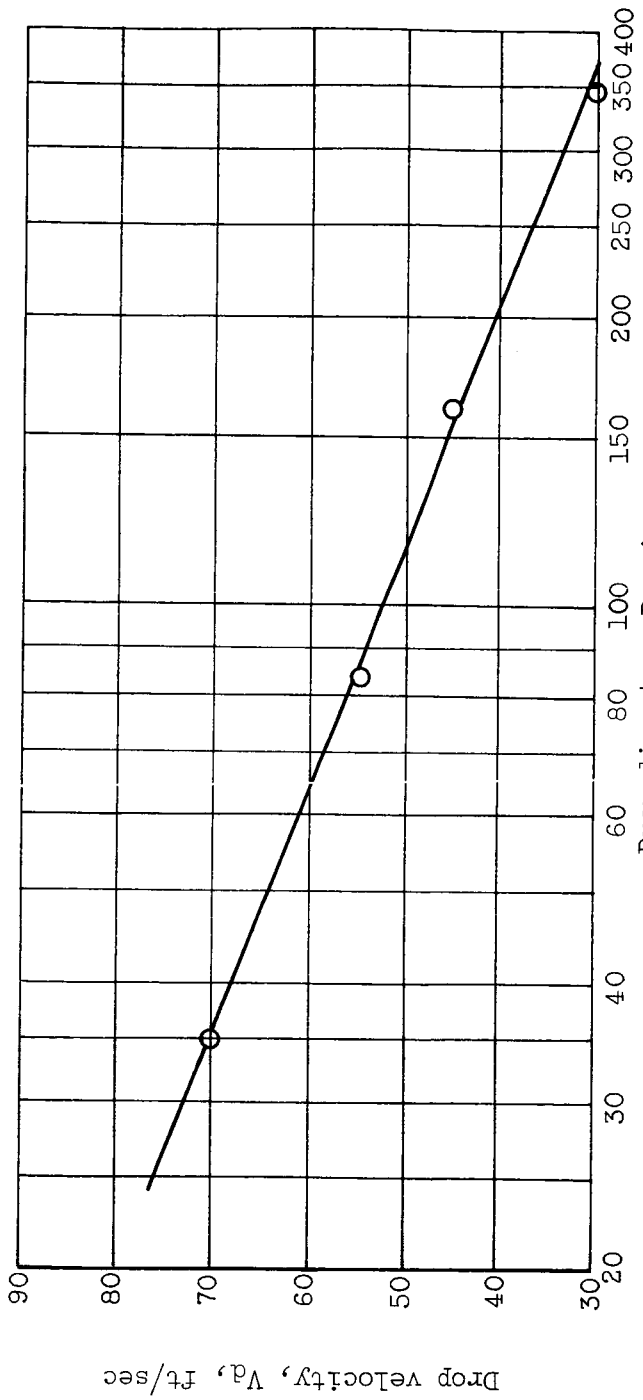


Figure 7. - Drop size and velocity data.

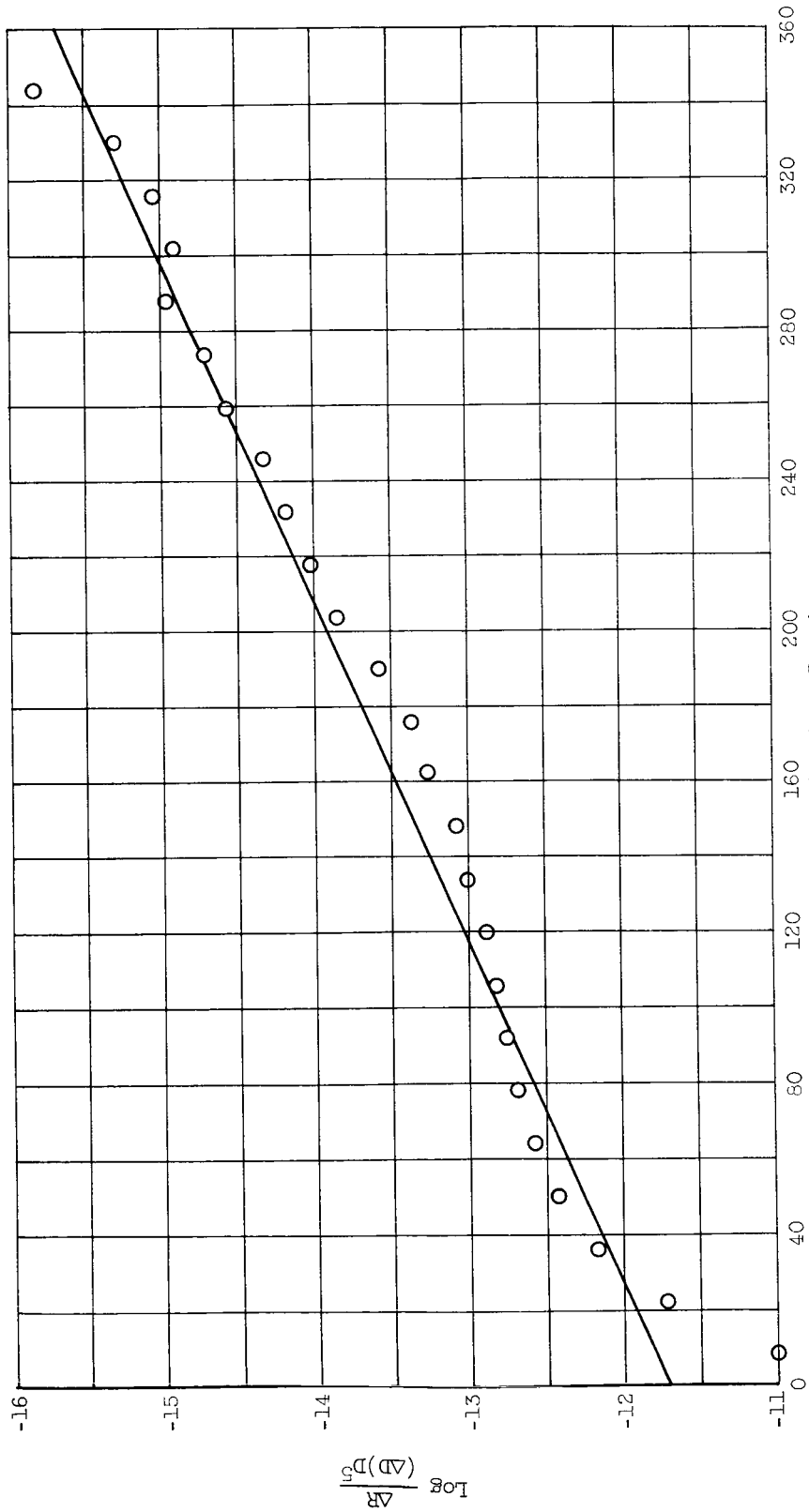


Figure 8. - Nukiyama-Tanasawa analysis of experimental drop-size data; b = 0.0254 and $D_{30}$ = 154 microns.

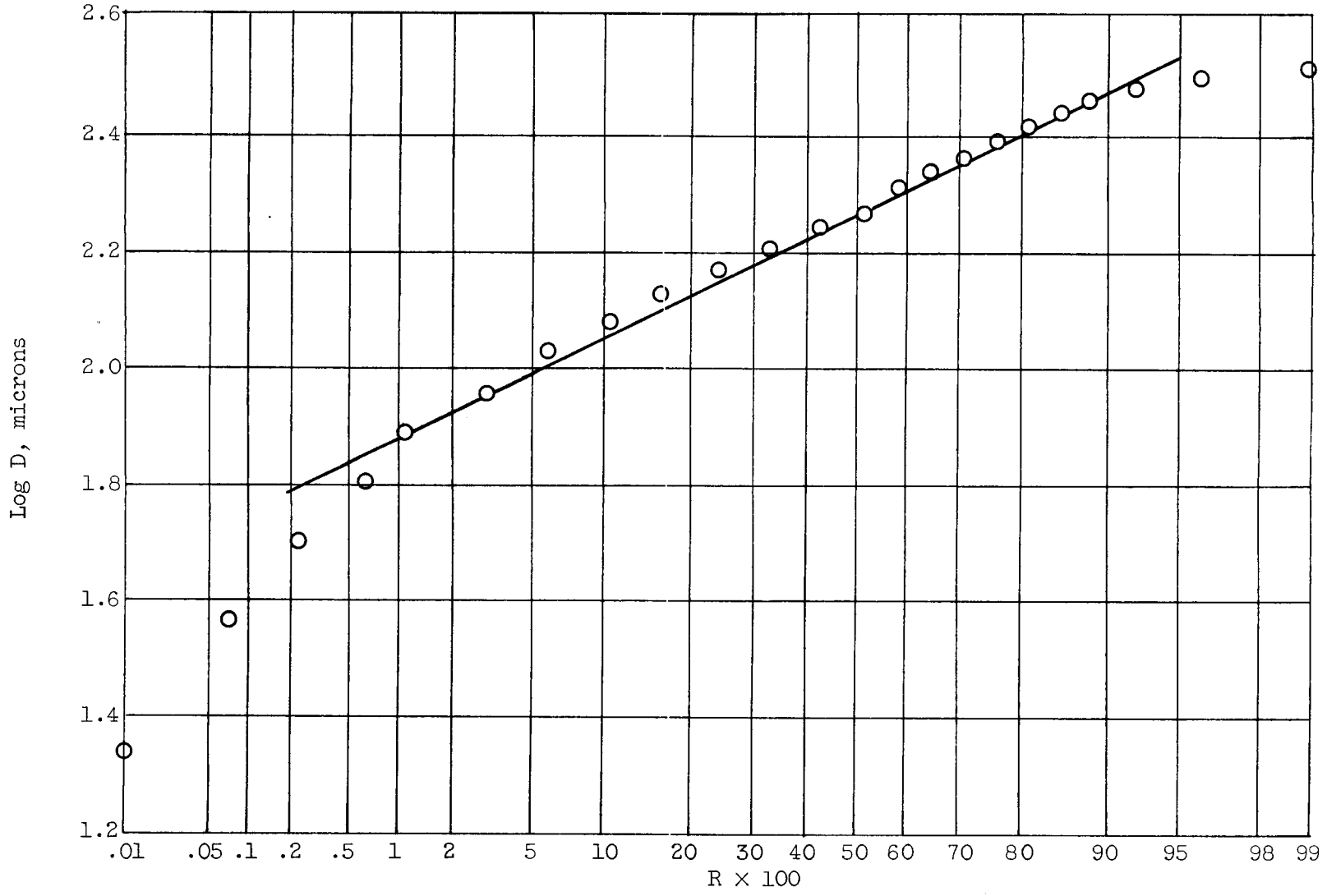


Figure 9. - Log-probability analysis; $D^*$ = 187 microns and $D_{30}$ = 158 microns.

Figure 10. - Rosin-Rammler analysis; $q = 3.2$, $\overline{D} = 288$ microns, and $D_{30} = 116$ microns.



NASA - Langley Field, Va.